

OXIDATIVE STRESS AND APOPTOSIS IN HOMOCYSTINURIA PATIENTS WITH GENETIC REMETHYLATION DEFECTS

Eva Richard^{1*}, Lourdes R. Desviat¹, Magdalena Ugarte¹ and Belén Pérez¹

¹Centro de Diagnóstico de Enfermedades Moleculares, Centro de Biología Molecular “Severo Ochoa” CSIC-UAM, Departamento de Biología Molecular. Universidad Autónoma de Madrid, Centro de Investigación Biomédica en Red de Enfermedades Raras (CIBERER), IdiPAZ, Madrid, Spain.

*Correspondence to: Dr. Eva Richard, PhD, Centro de Biología Molecular “Severo Ochoa”. Laboratorio 204. C/ Nicolás Cabrera Nº 1. Universidad Autónoma de Madrid, 28049 Madrid, Spain. Phone: +34911964596. Fax: +34911964420. E-mail: erichard@cbm.uam.es

RUNNING HEAD: Oxidative stress in homocystinuria patients

KEYWORDS: **Homocysteine; homocystinuria; remethylation; ROS; apoptosis; shRNA; stress-kinases.**

Total number of text figures: 6 figures

Total number of tables: 2 tables

Grant sponsor: Ministerio de Ciencia e Innovación of Spain; Grant number: SAF2010-15284.

ABSTRACT

Oxidative stress has been described as a putative disease mechanism in pathologies associated with an elevation of homocysteine. An increased reactive oxygen species (ROS) production and apoptosis rate have been associated with several disorders of cobalamin metabolism, particularly with methylmalonic aciduria combined with homocystinuria *cblC* type. In this work, we have evaluated several parameters related to oxidative stress and apoptosis in fibroblasts from patients with homocystinuria due to defects in the *MTR*, *MTRR* and *MTHFR* genes involved in the remethylation pathway of homocysteine. We have also evaluated these processes by knocking down the *MTRR* gene in cellular models, and complementation by transducing the wild-type gene in *cblE* mutant fibroblasts. All cell lines showed a significant increase in ROS content and in MnSOD expression level, and also a higher rate of apoptosis with similar levels to the ones in *cblC* fibroblasts. The amount of the active phosphorylated forms of p38 and JNK stress-kinases was also increased. ROS content and apoptosis rate increased in control fibroblasts and in a glioblastoma cell line by shRNA-mediated silencing of *MTRR* gene expression. In contrast, wild-type *MTRR* gene corrected mutant cell lines showed a decrease in ROS and apoptosis levels. To the best of our knowledge, this study provides the first evidence that an impaired remethylation capacity due to low *MTRR* and *MTR* activity might be partially responsible for stress response.

INTRODUCTION

Remethylation disorders are rare inherited metabolic diseases of enzymes involved in the remethylation of homocysteine to methionine causing homocystinuria. They include defects in methionine synthase (MTR, OMIM ID: 156570), methionine synthase reductase (MTRR, OMIM ID: 602568) and MMADHC (OMIM ID: 611935) proteins corresponding to *cblG*, *cblE* and *cblD-variant 1* cobalamin complementation groups respectively; and in 5,10-methylene tetrahydrofolate reductase enzyme (MTHFR, OMIM ID: 236250) [Watkins and Rosenblatt, 2011]. MTR protein is a methylcobalamin-dependent enzyme that catalyzes the successive transfer of a methyl group from 5-methyltetrahydrofolate to the cob(I)alamin form of the cofactor and from methylcobalamin to homocysteine to form methionine and tetrahydrofolate as products [Watkins et al., 2002] (Fig. 1). Activity of MTR depends on the presence of a second protein, MTRR, which reductively reactivates oxidized MTR and functions to maintain it in an active form [Leclerc et al., 1998]. When cobalamin becomes oxidized, MTRR catalyzes its reductive methylation, using S-adenosylmethionine (SAM) as a methyl donor to regenerate methylcobalamin (Fig. 1). SAM is an important methyl donor for many other cellular processes including DNA methylation, neurotransmitter synthesis and phospholipid metabolism. MTHFR is a cytosolic enzyme that catalyzes the reduction of 5,10-methylene tetrahydrofolate to 5-methyl tetrahydrofolate, the primary form of folate, which is utilized for homocysteine remethylation to methionine [Watkins and Rosenblatt, 2011] (Fig. 1).

Biochemically, these disorders are characterized by homocysteine elevation and low-to-normal methionine levels, without urinary methylmalonic acid excretion. Patients present severe clinical symptoms which are mainly neurological for MTHFR deficiency and neurohematological for *cblE* and *cblG* defects [Watkins and Rosenblatt,

2011]. The features vary with age of onset that ranges from the neonatal period to adulthood. Patients with neonatal disease exhibit acute neurological distress. Children and adults may experience acute or rapidly progressive neurological deterioration [Schiff et al., 2011]. To date, the biochemical goal for treatment of remethylation disorders is to decrease plasma homocysteine levels and to increase plasma methionine levels by augmenting residual methionine synthase activity with B₁₂. Vitamins B₉ and B₆ as well as betaine and methionine supplementation can also be provided to improve metabolic parameters [Schiff et al., 2011].

Two major mechanisms have been proposed to explain the pathogenesis of these diseases: i) defective methionine synthesis (with a consequent drop in SAM production and deficiencies of numerous methylation reactions leading to hypomyelination in the central nervous system) [Surtees, 1998] and ii) hyperhomocysteinemia or homocystinuria. MTHFR deficient mice exhibited hyperhomocysteinemia and decreased methylation capacity, with neuropathology and aortic lipid deposition [Chen et al., 2001; Chen et al., 2005]. MTRR knockout mice presented metabolic derangement of methionine and folate metabolism [Elmore et al., 2007].

Elevated homocysteine concentration has been proposed as a risk factor for numerous diseases, including neural tube defects, cardiovascular diseases and a range of neurodegenerative conditions [Zou and Banerjee, 2005]; and it has been suggested to induce neurological dysfunction via oxidative stress [Ho et al., 2001; James et al., 2004]. In addition, an increased reactive oxygen species (ROS) production and apoptosis induction in neurons [Zou et al., 2010], and in several tissues such as bone and vascular endothelium have been described due to elevated levels of homocysteine [Kim et al., 2006; Koh et al., 2006; Perna et al., 2003]. Our previous data support the role of oxidative stress in the pathophysiology of defects in cobalamin metabolism,

especially from patients with isolated methylmalonic aciduria (MMA) *cblB* type [Richard et al., 2007; Richard et al., 2006] and with MMA combined with homocystinuria (MMACHC) *cblC* type [Jorge-Finnigan et al., 2010; Richard et al., 2009]. We have also shown differences between *cblB* and *cblC* patient cells regarding the apoptosis rate and preferred apoptotic pathway: apoptosis appears to be mainly triggered through the extrinsic pathway in *cblC*, while the intrinsic pathway was primarily activated in *cblB* cells [Jorge-Finnigan et al., 2010]. Taking these observations into account, we hypothesized that homocysteine might be responsible for the differences observed between cells from patients with MMA (*cblB* type) and with MMACHC (*cblC* type) and might have a relevant role in oxidative stress and apoptosis processes in patients with these inherited metabolic diseases, as has been described in other diseases.

In order to study a different metabolic disorder in which homocysteine has a relevant role and to gain better insights into its pathophysiology, the purpose of this study has been to analyze several parameters related to stress response in fibroblasts from patients with homocystinuria caused by defects in the remethylation pathway along with the evaluation of these processes by knocking down the *MTRR* gene in cellular models and by expressing this gene in mutant cells. The data indicate that the impaired remethylation capacity in patients might be at least partly responsible for enhancing ROS and apoptosis levels.

MATERIALS AND METHODS

SAMPLES

The study included available fibroblasts from three patients belonging to *cblE* group (P1, P2 and P3) and one to *cblG* (P4); and from a patient with defects in the *MTHFR* gene (P5). Patients presented a high concentration of homocysteine in plasma ($>100 \mu\text{mol/l}$). Patients were referred from clinics to be biochemically and/or genetically diagnosed at Centro de Diagnóstico de Enfermedades Moleculares (CEDEM) in Madrid. Relevant clinical and molecular data about individual patients included in this study are detailed in Table 1. Genetic analysis of the family members showed that changes cosegregated in the respective families. The uniparental disomy causing homozygosity for the pathogenic mutation identified in P1 has been recently described [Pérez et al., 2012]. Skin fibroblasts from four controls (GM08333 (C1), GM08680 (C2), GM08429 (C3) and GM03348 (C4)) aged 2-10 years were obtained from Coriell Cell Repositories (NJ, USA). Fibroblast cultures were established from patient skin biopsies and cultivated according to standard procedures [Richard et al., 2007]. Assays were performed when the culture reached 75 to 85% confluence. Control and patient fibroblast cells were between passages 7 and 10. U87 human glioblastoma and SH-SY5Y human neuroblastoma cell lines were maintained in DMEM containing 10% FCS. Primary cultures of neurons from mice cortex were provided by Dr. F. Hernández, UAM, Madrid, Spain. Written informed consent to be included in this study was obtained from all subjects or their parents/legal guardians. Ethical approval for the use of human samples in the study was granted by the Ethics Committee of the Universidad Autónoma de Madrid.

ROS AND APOPTOSIS ASSAYS

Intracellular ROS and apoptotic cells were detected and quantitated by flow cytometry in fibroblasts as described [Richard et al., 2009].

Mitochondrial superoxide was detected using the red MitoSOXTM indicator (Invitrogen, Carlsbad, CA, USA). Cells were incubated with 5 μ M MitoSOXTM for 10 min at 37°C, protected from light. The measurements were carried out using FACSCantoII (BD Biosciences, San Jose, CA, USA).

WESTERN BLOT ANALYSIS

Total protein extracts were obtained from fibroblasts and glioblastoma cells for mitochondrial superoxide dismutase (MnSOD) and MTRR protein expression analysis as described [Richard et al., 2006]. For immunoblotting detection, samples (20 μ g total protein extracts) were loaded onto 4-12% NuPAGE Novex Bis-Tris mini gels (Invitrogen) and blotted onto nitrocellulose membranes using iBlot Dry Blotting system (Invitrogen). Western Blotting was carried out using anti- MnSOD (Enzo Life Science, PA, USA) diluted 1:5000 and anti-MTRR polyclonal antibody (Aviva Systems Biology, San Diego, CA, USA) diluted 1:1000. The stripped blots were reprobed with anti- α -tubulin antibody (1:5000, Cell Signaling Technology, Inc., Danvers, MA, USA). Anti-rabbit (MnSOD and MTRR detection) and anti-mouse (α -tubulin detection) secondary antibodies were used as IgG-horseradish peroxidase conjugated and were detected by Enhanced Chemiluminescence (GE, Healthcare, Berkshire, UK).

The activation of p38 and JNK stress kinases was analysed by Western Blot as previously described [Jorge-Finnigan et al., 2010]. The expression pattern of phosphorylated p38 and JNK proteins was individually normalized by the protein expression of total p38 and total JNK proteins which include both the phosphorylated (active) and unphosphorylated (inactive) forms.

shRNA/LENTIVIRUS INFECTION

Lentivirus incorporating shRNAs were generated in HEK293T packaging cells by cotransfection with pLKO.1 plasmid containing shRNA sequences (Sigma-Aldrich, St. Louis, MO, USA), packing plasmid pCMV-dR8.74, and envelope plasmid pMD2.G (both kindly provided by Dr. J. Diaz-Nido, UAM, Madrid, Spain) using lipofectamine and Plus reagent (Invitrogen, Carlsbad, CA, USA). Medium containing viral particles (non-target control shRNA (SHC002) or either of the *MTRR* shRNAs targeting different sequences of human *MTRR*) was harvested at 48 h after transfection and used to infect control fibroblasts with 4 µg/ml polybrene and U87 glioblastoma cells. Successfully infected cells were selected and maintained with 1 µg/ml puromycin (Sigma-Aldrich). shRNA clone information: clone TRC number: TRCN0000035404, TRCN0000035405, TRCN0000035406 and TRCN0000035407; clone ID: NM_002454.1-285s1c1, NM_002454.1-1310s1c1, NM_002454.1-1818s1c1 and NM_002454.1-549s1c1; clone sequence in http://www.sigmaaldrich.com/catalog/mission/SHCLNG-NM_002454?lang=es®ion=ES).

REAL-TIME PCR

Total RNA was isolated from control fibroblasts and U87 glioblastoma cells using MagNA Pure Compact RNA Isolation kit and MagNA Pure Compact instrument (Roche Applied Science, Mannheim, Germany). Samples were quantitated spectrophotometrically at 260 nm using the Nanodrop ND-1000 photometer (Thermo Scientific, Wilmington, MA, USA). The optimal design of the real-time PCR primers and the Universal ProbeLibrary probe selection was performed using ProbeFinder software (Roche Applied Science). RT-PCR was performed using GeneAmpPCRSysm9700 (Applied Biosystems, Carlsbad, CA, USA), and real-time PCR was performed using LightCycler 480 (Roche Applied Science), both from Unidad

de Genómica, Parque Científico de Madrid, UAM, Madrid, Spain. Amplification efficiency and sample-to-sample variation were normalized by monitoring GAPDH.

EXPRESSION OF HUMAN *MTRR* cDNA IN FIBROBLAST CELLS

Wild-type *MTRR* cDNA was cloned into a green fluorescent protein (GFP)-expressing pEZ-Lv201-lentiviral vector (EX-T8826-Lv201) (Source BioScience LifeSciences, Cambridge, UK). The empty lentiviral vector expressing GFP alone was used as control. Lentiviruses were generated by transient co-transfection with the lentiviral vectors, pCMV-dR8.74 and pMD2.G plasmids using lipofectamine and Plus reagent (Invitrogen) in HEK293T packaging cells. Lentiviruses encoding both GFP and *MTRR* proteins, or GFP alone were used to infect fibroblasts from P2 and P3 *cblE* patients. GFP expression in infected cells was ~70-90%, therefore GFP expressing-cells were not sorted. Mitochondrial superoxide and apoptosis assays were performed in the total cell population, but data analysis of these assays were carried out in GFP-positive cells also expressing *MTRR* protein.

RESULTS

Several parameters related to oxidative stress and cell death were evaluated in fibroblasts from 5 patients with homocystinuria (Table 1). First, we examined ROS levels in control and patient fibroblasts by flow cytometry (Table 2). There was a ~3-fold increase in ROS production in fibroblasts from all patients (Fig. 2A). We also evaluated the expression pattern of the mitochondrial MnSOD by Western Blot analysis. As shown in Figure 2B, the expression of MnSOD protein was increased in patient cells (~3-5-fold by densitometric analysis).

We next analysed the percentage of annexin V-positive apoptotic cells in patient fibroblasts. Flow cytometry analysis demonstrated elevated levels of annexin V-positive apoptotic cells (~2-3-fold) suggesting an increased basal level of apoptosis (Table 2 and Fig. 3A). Particularly, *cblE* patient P2 showed a three-fold increase compared to controls.

The activation of two proteins belonging to the mitogen-activated protein kinase (MAPK) superfamily, p38 kinase and Jun N-terminal kinase (JNK) was investigated by immunoblotting (Fig. 3B). A significantly increased expression of phospho-p38 and phospho-JNK (active forms) was detected in patient fibroblasts. Quantitative densitometric analysis demonstrated a 1.5-3-fold higher expression for phospho-p38; and a lower activation of JNK (1.2-2.5-fold) in patient cells compared to controls.

We also applied shRNA technology to stably knock down *MTRR* gene expression in control fibroblasts, as a representative gene involved in the remethylation pathway of homocysteine. After infection of control fibroblasts with lentivirus containing four different *MTRR* shRNAs or control shRNA and puromycin selection, we successfully obtained *MTRR* silenced cells in which their growth was not affected negatively in comparison to the non-target shRNA control. qRT-PCR was performed to

confirm gene-silencing effects at the mRNA level (Fig. 4A). The different *MTRR* shRNAs resulted in reductions of 70% for shRNA04, 85% for shRNA05, 35% for shRNA06 and 45% for shRNA07. In addition, Western Blot technique showed a significant decrease in MTRR protein expression especially in shRNA04 and shRNA05 cells (Fig. 4B). To demonstrate if *MTRR* gene silencing has an effect in oxidative stress, we analysed ROS content in *MTRR* shRNA and non-target shRNA control cells by flow cytometry. Interestingly, the results showed that ROS levels are increased in those shRNA cells in which *MTRR* mRNA expression is highly reduced (shRNA04 and shRNA05) (Fig. 4C). Next, we analysed the percentage of annexin V-positive apoptotic cells in *MTRR*-silenced fibroblasts. shRNA06 and shRNA07 cells showed a low level of apoptosis. In contrast, shRNA04 and shRNA05 fibroblasts showed a 1.5-fold increase in apoptosis compared to control cells (Fig. 4D).

To examine the *MTRR*-silencing effect in other cellular models, MTRR protein expression was first analysed in U87 glioblastoma and SH-SY5Y neuroblastoma human cell lines. MTRR expression was detectable in U87 glioblastoma however we could detect no expression of the protein in neither neuroblastoma cells nor neuronal mice cells (data not shown), suggesting a probable glial expression of MTRR protein. In view of these observations, we then examined stable shRNAs knockdown of *MTRR* gene expression in U87 glioblastoma cells for ROS and apoptosis analysis. The efficiency of *MTRR* knockdown in stable *MTRR* shRNA glioblastoma cells was assessed at mRNA and protein levels by qRT-PCR and Western Blot analysis respectively. Three of the four *MTRR* shRNAs efficiently reduced MTRR mRNA and protein levels compared with vector control cell lines (shRNA04, shRNA05 and shRNA07) (Fig. 5A, B). To study the mechanisms regulating the effects of *MTRR* knockdown on ROS and apoptosis function in this cellular model, we examined once more the fluorescence of

H₂DCFDA and annexin V probes by flow cytometry. Stable shRNAs knockdown of *MTRR* significantly increased ROS levels (Fig. 5C) and apoptosis rate (Fig. 5D).

shRNA04 and shRNA05 glioblastoma cells showed the highest increase in ROS and apoptosis levels compared with vector shRNA control cells (~2-fold).

It is worth noting that the use of four different *MTRR* shRNAs has defined our study since cells infected with those *MTRR* shRNAs that provided the highest silencing of the gene, also induced the highest elevation of ROS and apoptosis levels in both fibroblast and glioblastoma cellular models.

Homocysteine levels were also measured in cell culture medium from *MTRR* shRNA fibroblasts and glioblastoma cells. We found an increase of ~1.5-fold of homocysteine in those shRNA cells' medium in which the *MTRR* gene expression was highly reduced (see the Supplementary Table 1 for more details).

Finally, to verify if the loss of function of MTRR is related to the observed oxidative stress and apoptosis, we analysed these processes in two *cbIE* patient cells infected with the wild-type *MTRR* cDNA using a lentiviral vector. Mean fluorescence intensity measurement by flow cytometry of mitochondrial superoxide MitoSOX probe showed a decrease in superoxide anion levels in the infected cells expressing MTRR protein compared to the infected cells expressing GFP alone. ROS levels were significantly reduced in P3 (37%) and slightly reduced in P2 (15%) mutant fibroblasts expressing MTRR protein (Fig. 6A). In addition, annexin V-positive apoptotic cells were decreased in the infected cells expressing MTRR protein compared to the infected cells expressing GFP alone. Apoptosis rate was decreased ~20% in P2 and P3 *cbIE* mutant cells expressing MTRR protein (Fig. 6B).

DISCUSSION

Homocystinuria is caused by inborn metabolic defects in the transsulphuration or remethylation pathways of homocysteine. Remethylation defects are inherited metabolic diseases characterized by defective methionine synthesis and homocystinuria. The pathogenesis of these disorders is far from being understood; a reduced supply of methionine and SAM, or some other downstream metabolites, and an elevation of homocysteine have been proposed as the major pathophysiological mechanisms.

Elevation of homocysteine has also been correlated with complex and multifactorial diseases, including neural tube defects, cardiovascular and neurodegenerative diseases. Several hypotheses have been proposed, including oxidative stress, endoplasmic reticulum stress, and alterations in signal transduction pathways and activation of inflammatory factors to explain the mechanisms underlying homocysteine mediated-pathophysiology of these diseases [Zou and Banerjee, 2005]. Homocysteine is readily oxidized in plasma to form homocystine and homocysteine mixed disulfides, representing the predominant forms of this amino acid in circulation [Zou and Banerjee, 2005], and it can also undergo autooxidation causing the disruption of redox homeostasis in vascular and neuronal cells [Obeid and Herrmann, 2006]. This oxidation has been correlated with ROS generation. Homocysteine can stimulate ROS formation in a number of different cell types, such as splenic B lymphocytes [Zhang et al., 2001], mesangial cells [Yang and Zou, 2003], monocytes [Zeng et al., 2003] and vascular smooth muscle cells [Liu et al., 2008]. Several reports have shown that homocysteine induces neuronal apoptosis by increasing levels of cytosolic calcium and ROS formation in neurons which may be a putative disease mechanism in neurodegenerative disorders [Zou et al., 2010]. Our previous results from the study of several parameters of oxidative stress and apoptosis in fibroblasts from patients with

defects in cobalamin metabolism revealed that *cblB* and *cblC* groups presented the highest ROS and apoptosis levels [Richard et al., 2007; Richard et al., 2009]. Both groups accumulate the toxic methylmalonic acid in mitochondria; whereas the *cblC* group, apart from this organic acid, accumulates the cytosolic metabolite homocysteine. These observations encouraged us to continue the research in patients with homocystinuria. We have shown a ROS over-production and an increased apoptosis level in fibroblasts from all patients with homocystinuria studied in this work (*cblE*, *cblG* and MTHFR deficiency). These observations along with the recent study in plasma of patients with classical homocystinuria [Vanzin et al., 2011] suggest that oxidative stress might participate, at least in part, in the pathophysiology of homocystinuria. The over-expression of a marker of mitochondrial ROS production, MnSOD protein, was also found in fibroblasts from patients with homocystinuria which may be a compensatory mechanism that counteracts the consequences of elevated ROS levels, as has been reported in other disorders [Filosto et al., 2002; Hu et al., 2005; Kunishige et al., 2003; Ohkoshi et al., 1995], in a *Mut*-knockout mice liver [Chandler et al., 2009] and in cells from different MMA patients [Richard et al., 2007]. Similarly, as compensatory mechanism increased levels of the antioxidant glutathione resulting from the elevation of homocysteine has been described [Mosharov et al., 2000]. In addition, the increase in ROS and apoptosis levels in stable *MTRR*-silenced control fibroblasts and glioblastoma cell line, and the decrease of these levels in *MTRR* gene corrected mutant cells lines suggest that the impaired remethylation due to low MTRR and MTR activity may play a relevant role in these processes.

Our study of the activation of essential signaling proteins, such as p38 and JNK which belong to the mitogen-activated protein kinases (MAPKs) family [Temkin and Karin, 2007] has provided essential information about the signal transduction pathways

that could be involved in the pathogenesis of homocystinuria. The activation of p38 and JNK kinases in cells from patients with this disease revealed a stimulation of these stress-sensing pathways which could be correlated with elevated ROS levels. The same has been described for endothelial cells, where MAPKs (p38), ERK1/2 and NF- κ B signaling pathways were activated by homocysteine-induced ROS [Zou and Banerjee, 2005]. Homocysteine promoted also a rapid increase in phosphorylation of p38 MAPK in microglia [Zou et al., 2010], in vascular smooth muscle cells [Akasaka et al., 2005] and monocytes [Zeng et al., 2003].

Neurological damage has been reported in patients with homocystinuria, and numerous studies in recent years have investigated the role of homocysteine as a cause of brain damage. Several studies have explored homocysteine transport in the brain: it may be produced within the brain itself [Obeid and Herrmann, 2006]; and it may cross the blood-brain barrier probably in both directions [Kamath et al., 2006]. The neurotoxic effects of homocysteine have been described in several studies [Obeid and Herrmann, 2006], and homocysteine has been found to induce neurological dysfunction via oxidative stress [Ho et al., 2001; James et al., 2004]. Children with cystathionine β -synthase (CBS) deficiency ($>100 \mu\text{M}$ of homocysteine) have shown a 10-fold increase in the concentration of homocysteine in cerebrospinal fluid [Surtees et al., 1997]. It is interesting to note that fibroblasts from a CBS deficient patient, with defects in the transsulphuration homocysteine pathway, also showed high ROS and apoptosis levels [Richard et al., 2009]. Further studies are needed to evaluate stress response in more CBS patients. Presumably, the pathophysiological mechanisms underlying neurological impairment are different between remethylation and transsulphuration deficiencies. Further analysis will provide a deeper insight into the effect of homocysteine and other

metabolites in the activation of apoptosis and/or ROS production in homocystinuria disorders.

Finally, the cytotoxicity of homocysteine has been reported to be mitigated by antioxidants like N-acetyl cysteine, vitamin E or C [Ho et al., 2001; Reis et al., 2002; Wyse et al., 2002]. Interestingly, a number of epidemiological studies have found a link between antioxidant uptake and a reduced incidence of dementia in Alzheimer's disease [Grundman et al., 2002]. Our promising results will be followed up with further studies focused on using antioxidants as a novel approach for treatment of homocystinuria metabolic diseases. The administration of exogenous antioxidants should be evaluated as tools for optimizing therapies because the outcome of these pathologies might be improved in an early intervention.

In summary, we provide the first evidence that cells from homocystinuria patients with defects in the remethylation pathway showed high ROS and apoptosis levels. Moreover, p38 and JNK MAPKs might be activated in a ROS-dependent manner in these patients which could be responsible for apoptosis activation. Cell dysfunction and death due to oxidative stress may contribute in part to the pathogenesis of these inherited metabolic disorders.

ACKNOWLEDGEMENTS

This work was supported by a grant from Ministerio de Ciencia e Innovación of Spain (SAF2010-15284). We thank Dr. J. Diaz-Nido for kindly providing HEK293T cells, pCMV-dR8.74 and pMD2.G plasmids, Dr. F. Hernández for kindly providing primary cultures of neurons from mice cortex and Dr. G.M. Palomo for her excellent technical assistance in lentivirus production and cell infection. The institutional grant from Fundación Ramón Areces to the Centro de Biología Molecular “Severo Ochoa” is gratefully acknowledged.

CONFLICT OF INTEREST

The authors declare that there are no conflicts of interest.

REFERENCES

- Akasaka K, Akasaka N, Di Luozzo G, Sasajima T, Sumpio BE. 2005. Homocysteine promotes p38-dependent chemotaxis in bovine aortic smooth muscle cells. *J Vasc Surg* 41:517-22.
- Chandler RJ, Zerfas PM, Shanske S, Sloan J, Hoffmann V, DiMauro S, Venditti CP. 2009. Mitochondrial dysfunction in mut methylmalonic acidemia. *Faseb J* 23:1252-61.
- Chen Z, Karaplis AC, Ackerman SL, Pogribny IP, Melnyk S, Lussier-Cacan S, Chen MF, Pai A, John SW, Smith RS, Bottiglieri T, Bagley P, Selhub J, Rudnicki MA, James SJ, Rozen R. 2001. Mice deficient in methylenetetrahydrofolate reductase exhibit hyperhomocysteinemia and decreased methylation capacity, with neuropathology and aortic lipid deposition. *Hum Mol Genet* 10:433-43.
- Chen Z, Schwahn BC, Wu Q, He X, Rozen R. 2005. Postnatal cerebellar defects in mice deficient in methylenetetrahydrofolate reductase. *Int J Dev Neurosci* 23:465-74.
- Elmore CL, Wu X, Leclerc D, Watson ED, Bottiglieri T, Krupenko NI, Krupenko SA, Cross JC, Rozen R, Gravel RA, Matthews RG. 2007. Metabolic derangement of methionine and folate metabolism in mice deficient in methionine synthase reductase. *Mol Genet Metab* 91:85-97.
- Filosto M, Tonin P, Vattei G, Spagnolo M, Rizzuto N, Tomelleri G. 2002. Antioxidant agents have a different expression pattern in muscle fibers of patients with mitochondrial diseases. *Acta Neuropathol (Berl)* 103:215-20.
- Grundman M, Grundman M, Delaney P. 2002. Antioxidant strategies for Alzheimer's disease. *Proc Nutr Soc* 61:191-202.
- Ho PI, Collins SC, Dhitavat S, Ortiz D, Ashline D, Rogers E, Shea TB. 2001. Homocysteine potentiates beta-amyloid neurotoxicity: role of oxidative stress. *J Neurochem* 78:249-53.

Hu Y, Rosen DG, Zhou Y, Feng L, Yang G, Liu J, Huang P. 2005. Mitochondrial manganese-superoxide dismutase expression in ovarian cancer: role in cell proliferation and response to oxidative stress. *J Biol Chem* 280:39485-92.

James SJ, Cutler P, Melnyk S, Jernigan S, Janak L, Gaylor DW, Neubrandner JA. 2004. Metabolic biomarkers of increased oxidative stress and impaired methylation capacity in children with autism. *Am J Clin Nutr* 80:1611-7.

Jorge-Finnigan A, Gamez A, Perez B, Ugarte M, Richard E. 2010. Different altered pattern expression of genes related to apoptosis in isolated methylmalonic aciduria cblB type and combined with homocystinuria cblC type. *Biochim Biophys Acta* 1802:959-67.

Kamath AF, Chauhan AK, Kisucka J, Dole VS, Loscalzo J, Handy DE, Wagner DD. 2006. Elevated levels of homocysteine compromise blood-brain barrier integrity in mice. *Blood* 107:591-3.

Kim DJ, Koh JM, Lee O, Kim NJ, Lee YS, Kim YS, Park JY, Lee KU, Kim GS. 2006. Homocysteine enhances apoptosis in human bone marrow stromal cells. *Bone* 39:582-90.

Koh JM, Lee YS, Kim YS, Kim DJ, Kim HH, Park JY, Lee KU, Kim GS. 2006. Homocysteine enhances bone resorption by stimulation of osteoclast formation and activity through increased intracellular ROS generation. *J Bone Miner Res* 21:1003-11.

Kunishige M, Mitsui T, Akaike M, Kawajiri M, Shono M, Kawai H, Matsumoto T. 2003. Overexpressions of myoglobin and antioxidant enzymes in ragged-red fibers of skeletal muscle from patients with mitochondrial encephalomyopathy. *Muscle Nerve* 28:484-92.

Leclerc D, Wilson A, Dumas R, Gafuik C, Song D, Watkins D, Heng HH, Rommens JM, Scherer SW, Rosenblatt DS, Gravel RA. 1998. Cloning and mapping of a cDNA

for methionine synthase reductase, a flavoprotein defective in patients with homocystinuria. *Proc Natl Acad Sci U S A* 95:3059-64.

Liu X, Luo F, Li J, Wu W, Li L, Chen H. 2008. Homocysteine induces connective tissue growth factor expression in vascular smooth muscle cells. *J Thromb Haemost* 6:184-92.

Mosharov E, Cranford MR, Banerjee R. 2000. The quantitatively important relationship between homocysteine metabolism and glutathione synthesis by the transsulfuration pathway and its regulation by redox changes. *Biochemistry* 39:13005-11.

Obeid R, Herrmann W. 2006. Mechanisms of homocysteine neurotoxicity in neurodegenerative diseases with special reference to dementia. *FEBS Lett* 580:2994-3005.

Ohkoshi N, Mizusawa H, Shiraiwa N, Shoji S, Harada K, Yoshizawa K. 1995. Superoxide dismutases of muscle in mitochondrial encephalomyopathies. *Muscle Nerve* 18:1265-71.

Pérez B, Nevado J, Lapunzina P, Gallego L, Pérez-Cerdá C, Merinero B, Ugarte M, Desviat LR. 2012. Segmental uniparental disomy leading to homozygosity for a pathogenic mutation in three recessive metabolic diseases. *Mol Genet Metab* 105:270-1.

Perna AF, Ingrosso D, De Santo NG. 2003. Homocysteine and oxidative stress. *Amino Acids* 25:409-17.

Reis EA, Zugno AI, Franzon R, Tagliari B, Matte C, Lammers ML, Netto CA, Wyse AT. 2002. Pretreatment with vitamins E and C prevent the impairment of memory caused by homocysteine administration in rats. *Metab Brain Dis* 17:211-7.

Richard E, Alvarez-Barrientos A, Perez B, Desviat LR, Ugarte M. 2007. Methylmalonic acidemia leads to increased production of reactive oxygen species and induction of apoptosis through the mitochondrial/caspase pathway. *J Pathol* 213:453-61.

Richard E, Jorge-Finnigan A, Garcia-Villoria J, Merinero B, Desviat LR, Gort L, Briones P, Leal F, Perez-Cerda C, Ribes A, Ugarte M, Perez B. 2009. Genetic and cellular studies of oxidative stress in methylmalonic aciduria (MMA) cobalamin deficiency type C (cblC) with homocystinuria (MMACHC). *Hum Mutat* 30:1558-66.

Richard E, Monteoliva L, Juarez S, Perez B, Desviat LR, Ugarte M, Albar JP. 2006. Quantitative analysis of mitochondrial protein expression in methylmalonic acidemia by two-dimensional difference gel electrophoresis. *J Proteome Res* 5:1602-10.

Schiff M, Benoist JF, Tilea B, Royer N, Giraudier S, Ogier de Baulny H. 2011. Isolated remethylation disorders: do our treatments benefit patients? *J Inherit Metab Dis* 34:137-45.

Surtees R. 1998. Demyelination and inborn errors of the single carbon transfer pathway. *Eur J Pediatr* 157 Suppl 2:S118-21.

Surtees R, Bowron A, Leonard J. 1997. Cerebrospinal fluid and plasma total homocysteine and related metabolites in children with cystathionine beta-synthase deficiency: the effect of treatment. *Pediatr Res* 42:577-82.

Temkin V, Karin M. 2007. From death receptor to reactive oxygen species and c-Jun N-terminal protein kinase: the receptor-interacting protein 1 odyssey. *Immunol Rev* 220:8-21.

Vanzin CS, Biancini GB, Sitta A, Wayhs CA, Pereira IN, Rockenbach F, Garcia SC, Wyse AT, Schwartz IV, Wajner M, Vargas CR. 2011. Experimental evidence of oxidative stress in plasma of homocystinuric patients: a possible role for homocysteine. *Mol Genet Metab* 104:112-7.

Watkins D, Rosenblatt, DS. 2011. Inherited disorders of folate and cobalamin transport and metabolism. In: Scriver CR, Beaudet AL, Sly W, Valle D, editors: *The Metabolic and Molecular Bases of Inherited Diseases*. New York: McGrall-Hill. p 3897-3933.

Watkins D, Ru M, Hwang HY, Kim CD, Murray A, Philip NS, Kim W, Legakis H, Wai T, Hilton JF, Ge B, Dore C, Hosack A, Wilson A, Gravel RA, Shane B, Hudson TJ, Rosenblatt DS. 2002. Hyperhomocysteinemia due to methionine synthase deficiency, cblG: structure of the MTR gene, genotype diversity, and recognition of a common mutation, P1173L. *Am J Hum Genet* 71:143-53.

Wyse AT, Zugno AI, Streck EL, Matte C, Calcagnotto T, Wannmacher CM, Wajner M. 2002. Inhibition of Na(+),K(+)-ATPase activity in hippocampus of rats subjected to acute administration of homocysteine is prevented by vitamins E and C treatment. *Neurochem Res* 27:1685-9.

Yang ZZ, Zou AP. 2003. Homocysteine enhances TIMP-1 expression and cell proliferation associated with NADH oxidase in rat mesangial cells. *Kidney Int* 63:1012-20.

Zeng X, Dai J, Remick DG, Wang X. 2003. Homocysteine mediated expression and secretion of monocyte chemoattractant protein-1 and interleukin-8 in human monocytes. *Circ Res* 93:311-20.

Zhang Q, Zeng X, Guo J, Wang X. 2001. Effects of homocysteine on murine splenic B lymphocyte proliferation and its signal transduction mechanism. *Cardiovasc Res* 52:328-36.

Zou CG, Banerjee R. 2005. Homocysteine and redox signaling. *Antioxid Redox Signal* 7:547-59.

Zou CG, Zhao YS, Gao SY, Li SD, Cao XZ, Zhang M, Zhang KQ. 2010. Homocysteine promotes proliferation and activation of microglia. *Neurobiol Aging* 31:2069-79.

FIGURE LEGENDS

Figure 1. Remethylation pathway of homocysteine. MTRR: methionine synthase reductase, responsible for the *cblE* disorder; MeCbl: methylcobalamin; MTR: methionine synthase, affected in the *cblG* disorder; MTHFR: methylene tetrahydrofolate reductase; SAM: S-adenosylmethionine; SAHCy: S-adenosylhomocysteine.

Figure 2. Analysis of intracellular ROS levels and MnSOD protein expression in control and patient fibroblasts. (A) ROS content was determined by flow cytometry using H₂DCFDA as a fluorescence probe. Results are expressed as DCF fluorescence relative to control cells. Control value was determined as the mean of data from the four control cell lines. Data represent mean values \pm standard deviation from at least three independent experiments, each one performed by triplicate (** $P < 0.01$). (B) Equal amounts from the four controls and patients were loaded (20 μ g of total cell lysates) and subjected to Western Blotting with anti-MnSOD antibody. The bottom panel shows the stripped blots reprobed with anti- α -tubulin antibody to ensure equal amounts of protein loaded in each lane. This result is representative of three independent experiments. Protein quantification was performed by laser densitometry. The ratios between MnSOD/ α -tubulin for each cell line were calculated to determine the expression fold-change relative to controls. Data represent mean \pm SD of three independent experiments (* $P < 0.05$; ** $P < 0.01$). (A and B) Patients along with the complementation groups they belong to are depicted in the figure. C: control; P: patient.

Figure 3. Analysis of apoptosis and phosphorylated p38 and JNK stress-activated protein kinases expression in control and patient fibroblasts. (A) Percentage of annexin V-positive apoptotic cells in patient and control cells relative to total cell number per sample by flow cytometry. Control value was determined as the mean of

data from the four control cell lines. Data represent mean \pm standard deviation of three independent experiments, each one performed by triplicate (* P < 0.05; ** P < 0.01). **(B)** Equal amounts from the four controls and patients were loaded (20 μ g of total cell lysates) and subjected to immunoblotting with anti-phosphorylated p38 and anti-phosphorylated JNK antibodies. The stripped blots were reprobbed with total anti-p38 and total anti-JNK antibodies as evidence of the equivalent amounts of protein loaded in each lane. The results in each case are representative of at least three independent experiments. Protein quantification was performed by laser densitometry. The ratios between phosphorylated/total kinase forms for each cell line were calculated to determine the activation fold-change relative to controls. Data represent mean \pm SD of three independent experiments (* P < 0.05; ** P < 0.01). **(A and B)** Patients along with the complementation groups they belong to are depicted in the figure. C: control; P: patient.

Figure 4. Results of shRNA knockdown in control fibroblasts. (A) Quantification of MTRR mRNA expression by qRT-PCR. Quantities are shown as % MTRR mRNA expression relative to fibroblasts infected with non-target control shRNA (shRNAc). The data represent mean \pm standard deviation of three independent experiments. **(B) Analysis of MTRR protein expression by Western Blot.** 50 μ g of total cell lysates were loaded and subjected to immunoblotting with anti-MTRR antibody. The bottom panel shows the stripped blot reprobbed with anti- α -tubulin antibody to ensure equal amounts of protein loaded in each lane. **(C) Detection of intracellular ROS levels.** ROS content was determined by flow cytometry using H₂DCFDA as fluorescence probe. Results are expressed as DCF fluorescence relative to non-target control shRNA (shRNAc). Data represent mean values \pm standard deviation from at least two independent experiments, each one performed by triplicate (* P < 0.05). **(D) Apoptosis detection by flow cytometry.** Percentage of annexin V-positive apoptotic cells in

MTRR shRNAs and non-target control shRNA (shRNAc) relative to total cell number per sample. Data represent mean \pm standard deviation of two independent experiments, each one performed by triplicate (* $P < 0.05$). (A, B, C and D) shRNA04, shRNA05, shRNA06 and shRNA07 indicate *MTRR* shRNAs targeting different sequences of human *MTRR* used in this study for the generation of lentiviral particles and infection of fibroblasts (see Materials and Methods).

Figure 5. Results of shRNA knockdown in U87 glioblastoma cells. (A)

Quantification of *MTRR* mRNA expression by qRT-PCR. Quantities are shown as % *MTRR* mRNA expression relative to U87 cells infected with non-target control shRNA (shRNAc). The data represent mean \pm standard deviation of three independent experiments. **(B) Analysis of *MTRR* protein expression by Western Blot.** 50 μ g of total cell lysates were loaded and subjected to immunoblotting with anti-*MTRR* antibody. The bottom panel shows the stripped blot reprobed with anti- α -tubulin antibody to ensure equal amounts of protein loaded in each lane. **(C) Detection of intracellular ROS levels.** ROS content was determined by flow cytometry using H₂DCFDA as fluorescence probe. Results are expressed as DCF fluorescence relative to non-target control shRNA (shRNAc). Data represent mean values \pm standard deviation from at least two independent experiments, each one performed by triplicate (* $P < 0.05$; ** $P < 0.01$). **(D) Apoptosis detection by flow cytometry.** Percentage of annexin V-positive apoptotic cells in *MTRR* shRNAs and non-target control shRNA (shRNAc) relative to total cell number per sample. Data represent mean \pm standard deviation of two independent experiments, each one performed by triplicate (* $P < 0.05$; ** $P < 0.01$). (A, B, C and D) shRNA04, shRNA05, shRNA06 and shRNA07 indicate the *MTRR* shRNAs targeting different sequences of human *MTRR* used in this study for the

generation of lentiviral particles and infection of U87 glioblastoma cells (see Materials and Methods).

Figure 6. Mitochondrial superoxide and apoptosis analysis in infected *cblE* patient cells expressing MTRR protein. (A) Mitochondrial superoxide detection by flow cytometry. Oxidative stress was measured by a mean intensity of fluorescence of MitoSOX in each infected cells expressing MTRR protein respect to the same cell line expressing GFP alone. Data represent mean \pm standard deviation of three independent experiments, each one performed by triplicate (* $P < 0.05$; ** $P < 0.01$). **(B) Apoptosis detection by flow cytometry.** Percentage of annexin V-positive apoptotic cells in infected cells expressing MTRR protein and GFP alone relative to total cell number per sample. Data represent mean \pm standard deviation of three independent experiments, each one performed by triplicate (* $P < 0.05$).

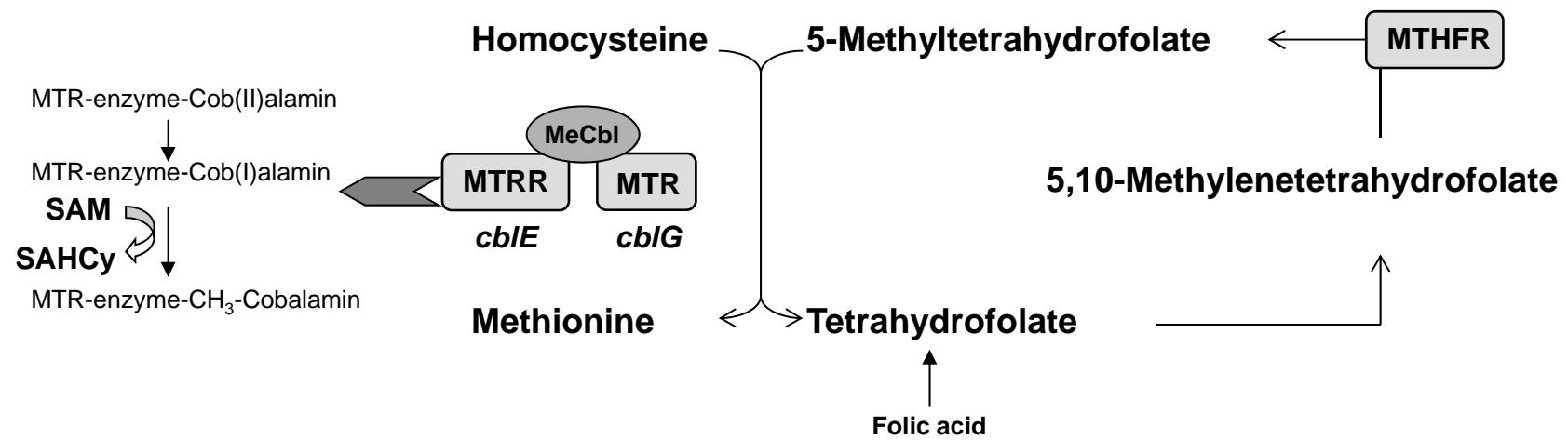
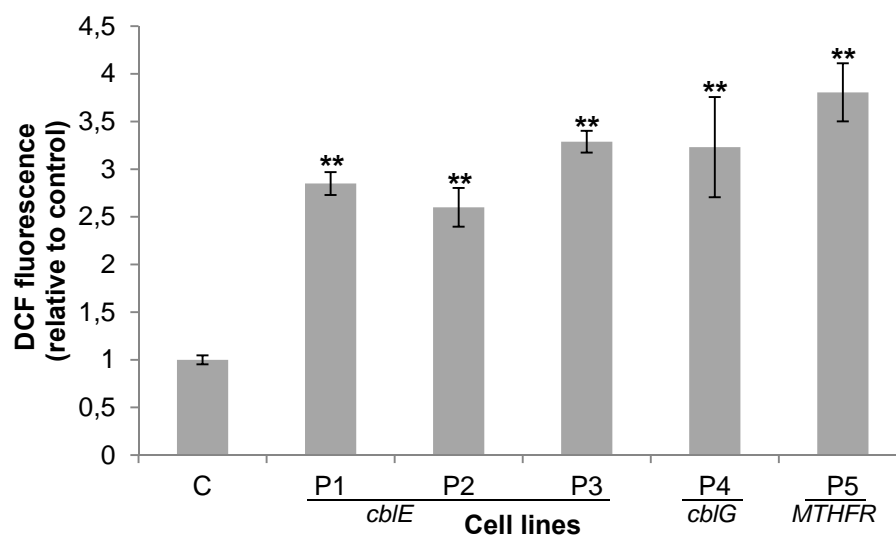


Figure 1

A



B

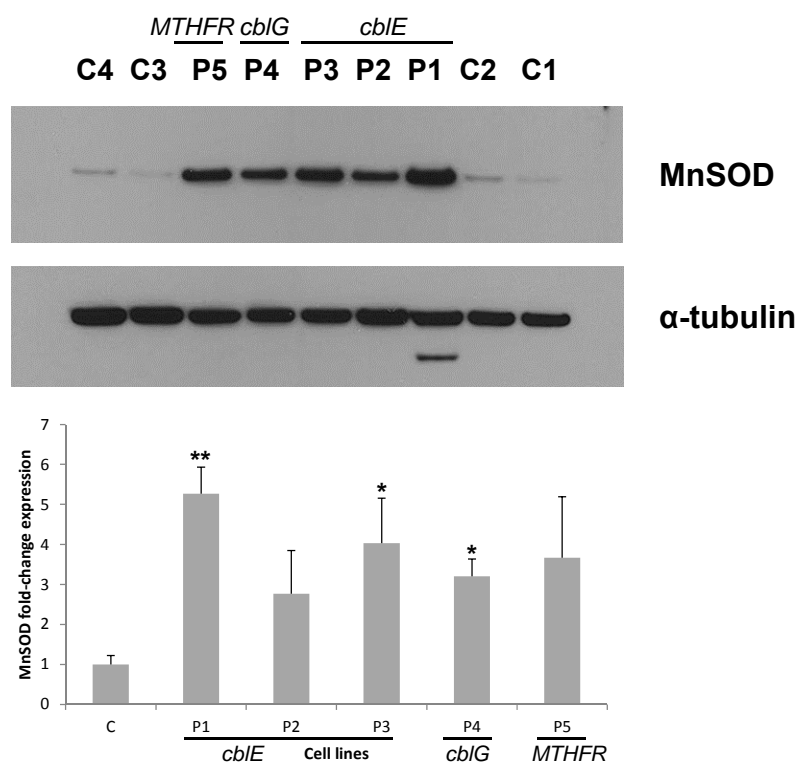
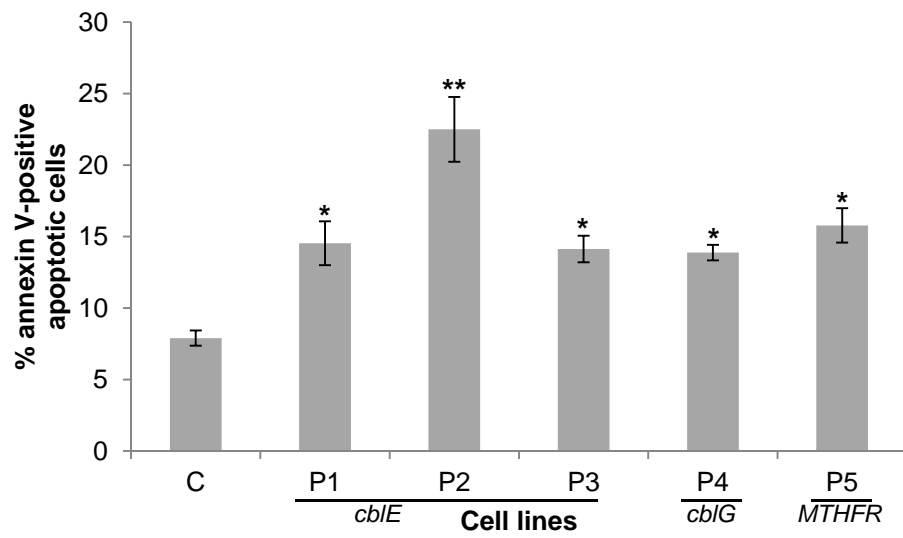


Figure 2

A



B

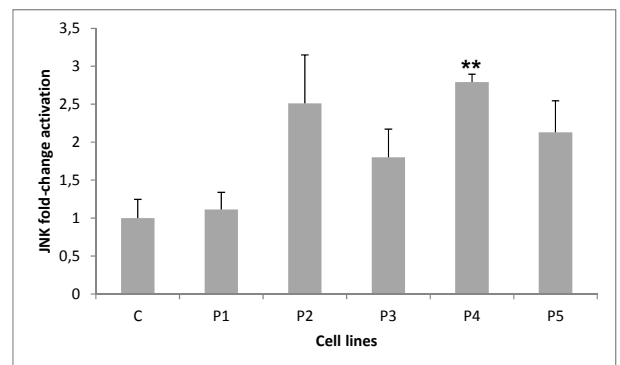
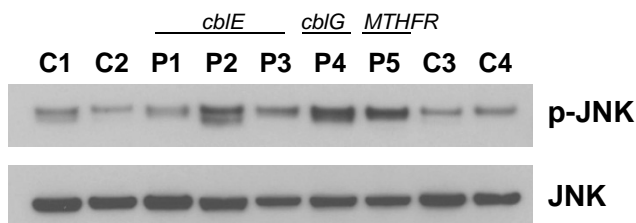
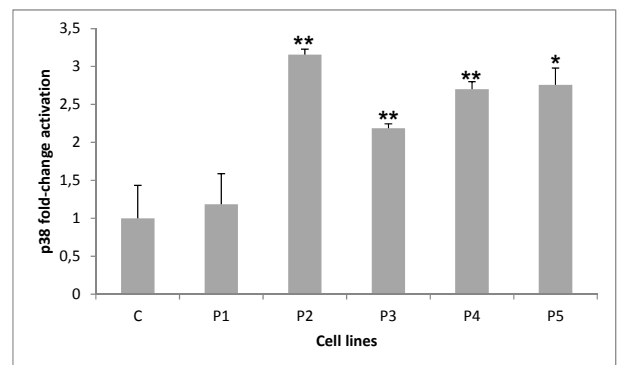
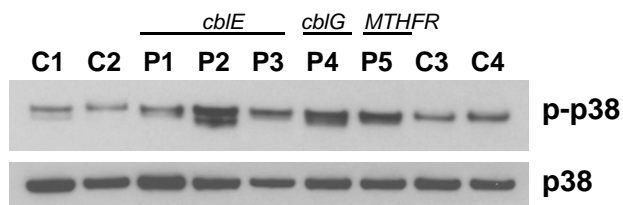
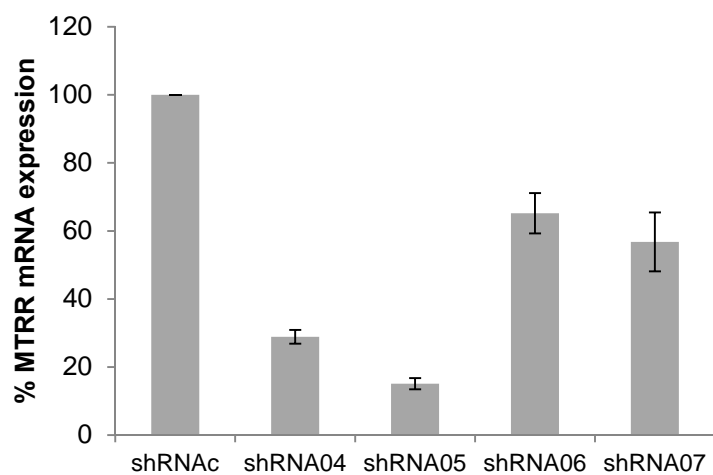
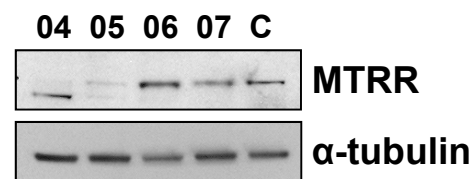
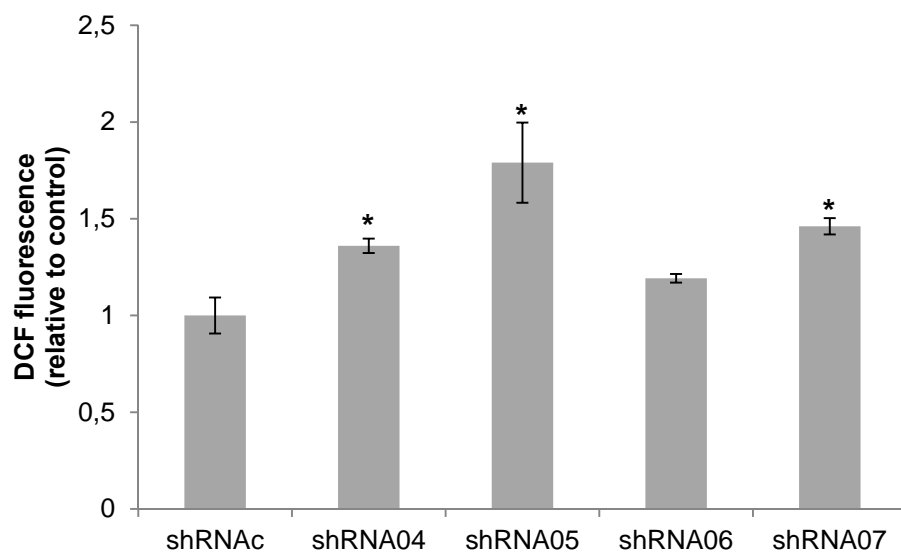
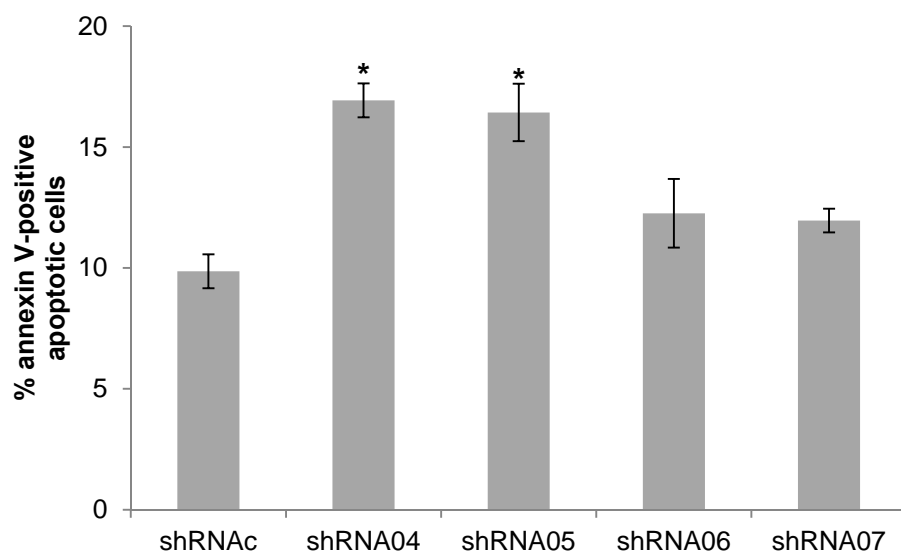
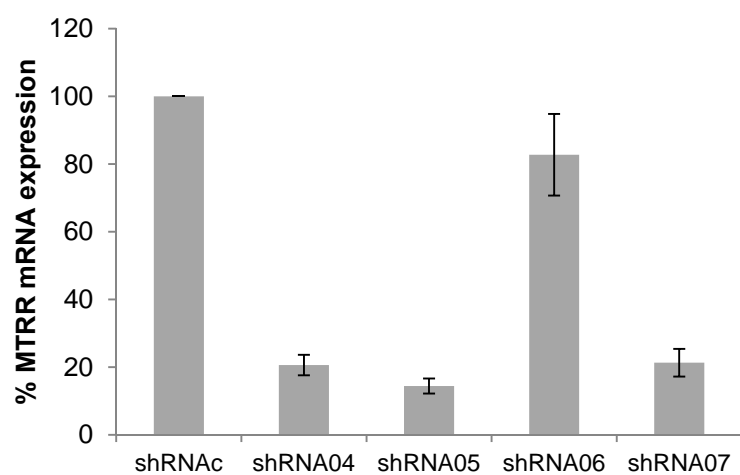
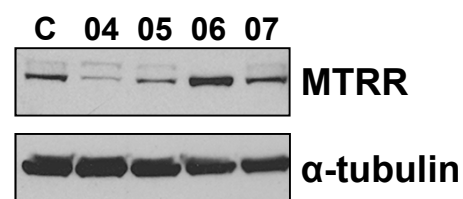
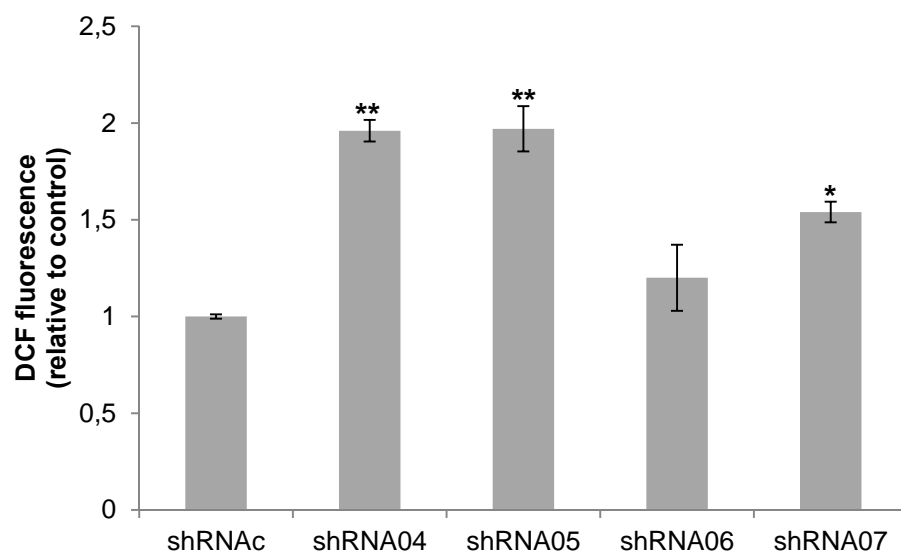
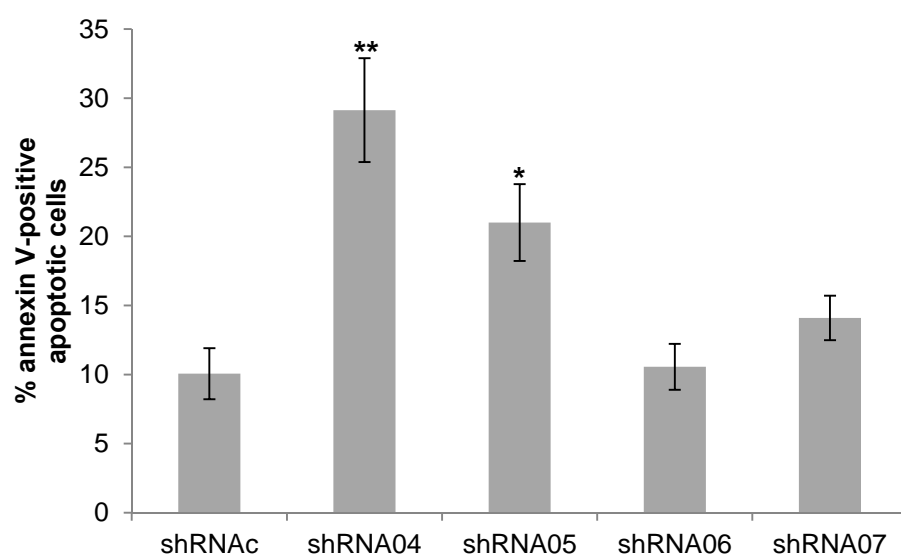


Figure 3

A**B****C****D****Figure 4**

A**B****C****D****Figure 5**

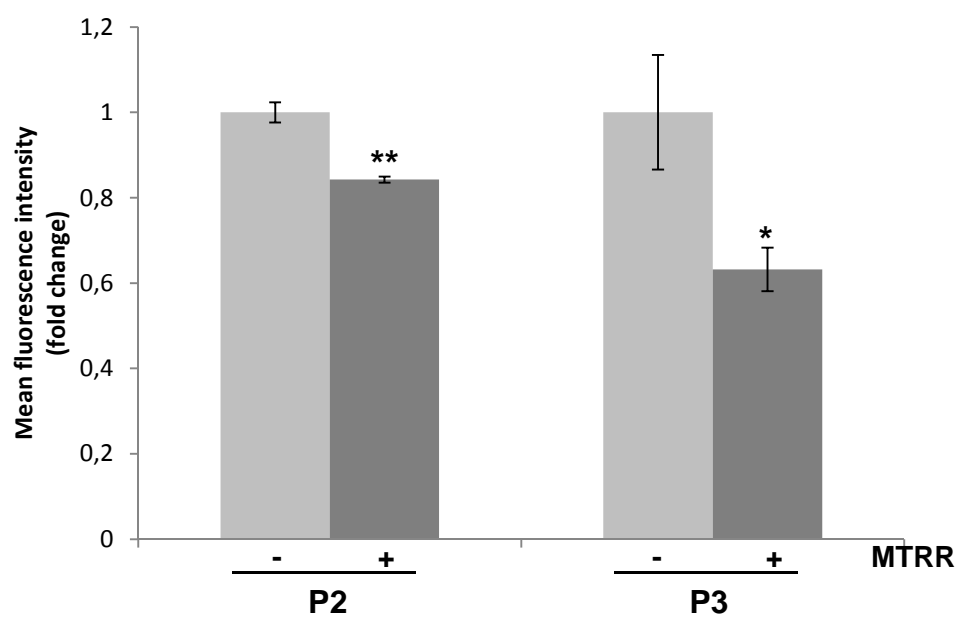
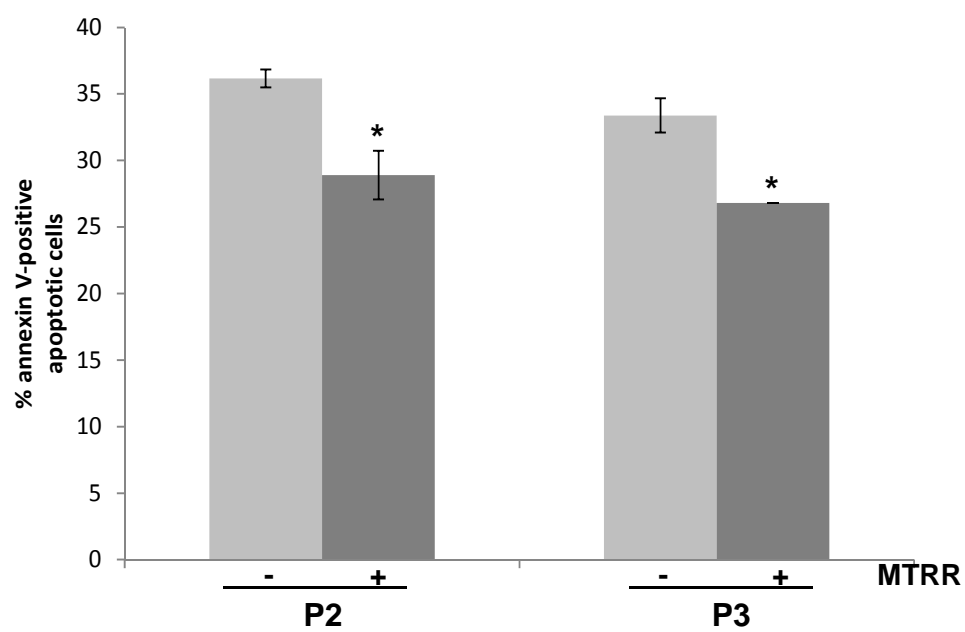
A**B**

Figure 6